Permutation entropy based time series analysis: equalities in the input signal can lead to false conclusions

Luciano Zunino[a,b,*], Felipe Olivares[c], Felix Scholkmann[d], Osvaldo A. Rosso[e,f,g]

[a] *Centro de Investigaciones Ópticas (CONICET La Plata - CIC), C.C. 3, 1897 Gonnet, Argentina*
[b] *Departamento de Ciencias Básicas, Facultad de Ingeniería, Universidad Nacional de La Plata (UNLP), 1900 La Plata, Argentina*
[c] *Instituto de Física, Pontificia Universidad Católica de Valparaíso (PUCV), 23-40025 Valparaíso, Chile*
[d] *Research Office for Complex Physical and Biological Systems (ROCoS), Mutschellenstr. 179, 8038 Zurich, Switzerland*
[e] *Instituto de Física, Universidade Federal de Alagoas (UFAL), BR 104 Norte km 97, 57072-970. Maceió, Alagoas, Brazil*
[f] *Instituto Tecnológico de Buenos Aires (ITBA) and CONICET, C1106ACD, Av. Eduardo Madero 399. Ciudad Autónoma de Buenos Aires, Argentina*
[g] *Complex Systems Group, Facultad de Ingeniería y Ciencias Aplicadas, Universidad de los Andes, Av. Mons. Álvaro del Portillo 12.455, Las Condes, Santiago, Chile*

Abstract

Permutation entropy is becoming a widely used concept in the field of nonlinear time series analysis. Its usefulness for characterizing the degree of regularity of complex time series is evidenced by the enormous amount of successful applications in diverse research areas. A symbolic encoding scheme, based on the ordinal relation between the amplitude of neighboring values of a given data sequence, needs to be implemented before estimating this entropic measure. Consequently, equalities in the analyzed signal, *i.e.* repeated equal values, deserve special attention and treatment. Two approaches have been suggested for overcoming this drawback, namely, to rank ties following their temporal order or to break them by adding small random perturbations. Since in most of applications the former alternative has been adopted, in this work, we carefully study the effect that the presence of equalities has on permutation entropy estimated values when these ties are symbolized according to their order of appearance. On the one hand, the analysis of computer-generated time series is initially developed to understand the incidence of repeated values on permutation entropy estimations in controlled scenarios. The presence of temporal correlations is erroneously concluded when true pseudorandom time series with low resolutions are considered. On the other hand, the analysis of real-world data is included to illustrate how the presence of a significant number of equal values can give rise to false conclusions regarding the underlying temporal structures in practical contexts. We consider that our findings can be useful for a more appropriate interpretation of results obtained using the permutation entropy and/or related ordinal symbolic quantifiers, especially when analyzing experimental time series digitized with low resolutions.

Keywords: Time series analysis; Permutation entropy; Equalities; Spurious temporal correlations

---

1. Introduction

Permutation entropy (PE) is becoming a a popular tool for the characterization of complex time series. Since its introduction almost fifteen years ago by Bandt and Pompe (BP) in their foundational paper [1], it has been successfully applied in a wide range of scientific areas and for a vast number of purposes. Without being exhaustive, applications in heterogeneous fields, such as biomedical signal processing and analysis [2–10], optical chaos [11–15], hydrology [16–18], geophysics [19–21], econophysics [22–25], engineering [26–29], and biometrics [30] can be mentioned. The PE is just the celebrated Shannon entropic measure evaluated using the ordinal scheme introduced by BP to extract the probability distribution associated with an input signal. This ordinal symbolic method, based on the relative amplitude of time series values, naturally arises from the time series (without any model assumptions) and inherits the causal information that stems from the temporal structure of the system dynamics. The relative frequencies of ordinal or permutation patterns, that quantify the temporal ranking information in the data sequence, need to be firstly calculated. Because of its definition via ordinal relationships, the way to handle equal amplitude values may have significant consequences when estimating the ordinal patterns probability

*Corresponding author

Email addresses: lucianoz@ciop.unlp.edu.ar (Luciano Zunino), olivaresfe@gmail.com (Felipe Olivares), Felix.Scholkmann@gmail.com (Felix Scholkmann), oarosso@gmail.com (Osvaldo A. Rosso)

distribution. In the case of variables with continuous distributions, ties can be simply ignored because they are very rare. However, experimental data digitized with relatively low resolutions could have a significant number of equalities and, consequently, the PE estimations may be affected by the procedure to consider them. Equal values in the time series are usually ranked according to their temporal order. The other recipe, suggested by BP [1], is to break ties by adding a small amount of noise. This second alternative has been rarely implemented. In this paper, we characterize the effect that the presence of equalities in the data sequence has on the PE estimations when the former, most used, approach is adopted. Through numerical and real-world data analyses, we demonstrate that the PE estimated values are biased as a consequence of the presence of equal values, and more regular dynamics than those expected can be erroneously concluded. We consider that this finding is relevant for a more appropriate interpretation of the results obtained when the PE is used for characterizing the underlying dynamics of experimentally acquired observables. In particular, the effect of ties should be especially considered when using the PE for comparing the regularity degree of two or more experimental datasets recorded with different sampling resolutions. Our main motivation is to warn future PE users about the importance to take this limitation into account for avoiding potential misunderstandings. Obviously, all related quantifiers estimated using the BP symbolic representation, *i.e.* with the symbolic method that considers the temporal ranking information (ordinal or permutation patterns) of the time series, can be also affected by this issue. We can enumerate permutation statistical complexity [31, 32], permutation directionality index [33], symbolic transfer entropy [34], Tsallis permutation entropy [35], Rényi permutation entropy [36, 37], conditional entropy of ordinal patterns [38], permutation min-entropy [39], multiscale permutation entropy measures [40], and time-scale independent permutation entropy [41], among many others. It is worth mentioning here that Bian *et al.* [42] have proposed the *modified* permutation-entropy (mPE) as an interesting alternative for dealing with equal values. Mapping equal values to the same symbols, these authors have shown that the mPE allows for an improved characterization of heart rate variability signals under different physiological and pathological conditions. However, Bian and co-authors' approach has a different physical interpretation and can not be considered as a *generalized* permutation entropy. For instance, the mPE does not reach its maximum value for a totally random signals (white noise) as this actually happens for the standard PE. Also the *weighted* permutation entropy (WPE) has been introduced by Fadlallah *et al.* [43] a couple of years ago as an improved PE by incorporating amplitude information. Through this weighted scheme, better noise robustness and distinctive ability to characterize data with spiky features or having abrupt changes in magnitude have been achieved. As it will be shown below, the presence of ties also has a significant incidence on WPE estimated values.

The remainder of the paper is organized as follows. In Section 2, the PE is introduced. A testbed analysis on computer-generated time series is included in Section 3 in order to understand the incidence of the presence of equal values on the PE estimations. Section 4 presents a couple of analyses of real-world data to illustrate this drawback in practical situations. Finally, in Section 5, the main conclusions reached in this work are summarized.

2. Permutation entropy

The PE has been introduced by BP as a natural complexity measure for time series [1]. It is the Shannon entropy of the ordinal symbolic representation obtained from the original sequence of observations. The idea behind ordinal pattern analysis is to consider order relations between values of time series instead of the values themselves. This ordinal symbolization is distinguished from other symbolic representations principally due to important practical advantages. Namely, it is conceptually simple, computationally fast, robust against noise, and invariant with respect to nonlinear monotonous transformations. Furthermore, the BP ordinal method of symbolization naturally arises from the time series, avoids amplitude threshold dependencies that affect other more conventional symbolization recipes based on range partitioning [44], and, perhaps more importantly, inherits the causal information that stems from the dynamical evolution of the system. As stated by Amigó *et al.* [45], "ordinal patterns are not symbols *ad hoc* but they actually encapsulate qualitative information about the temporal structure of the underlying data." Because of all these advantages, the

BP approach has been commonly implemented for revealing the presence of subtle temporal correlations in time series [39, 46–49].

Next, we summarize how to estimate the PE from a time series with a toy numerical example. Let us assume that we start with the time series $X = \{4, 1, 6, 5, 10, 7, 2, 8, 9, 3\}$. To symbolize the series into ordinal patterns, two parameters, the *embedding dimension* $D \geq 2$ ($D \in \mathbb{N}$, number of elements to be compared with each other) and the *embedding delay* τ ($\tau \in \mathbb{N}$, time separation between elements) should be chosen. The time series is then partitioned into subsets of length D with delay τ similarly to phase space reconstruction by means of time-delay-embedding. The elements in each new partition (of length D) are replaced by their rank in the subset. For example, if we set $D = 3$ and $\tau = 1$, there are eight different three-dimensional vectors associated with X. The first one $(x_0, x_1, x_2) = (4, 1, 6)$ is mapped to the ordinal pattern (102). The second three-dimensional vector is $(x_0, x_1, x_2) = (1, 6, 5)$, and (021) will be its related permutation. The procedure continues so on until the last sequence, $(8, 9, 3)$, is mapped to its corresponding motif, (120). Afterward, an ordinal pattern probability distribution, $P = \{p(\pi_i), i = 1, \ldots, D!\}$, can be obtained from the time series by computing the relative frequencies of the $D!$ possible permutations π_i. Continuing with the toy example: $p(\pi_1) = p(012) = 1/8$, $p(\pi_2) = p(021) = 1/4$, $p(\pi_3) = p(102) = 3/8$, $p(\pi_4) = p(120) = 1/8$, $p(\pi_5) = p(201) = 0$, and $p(\pi_6) = p(210) = 1/8$. The PE is just the Shannon entropy estimated by using this ordinal pattern probability distribution, $S[P] = -\sum_{i=1}^{D!} p(\pi_i) \log(p(\pi_i))$. Coming back to the example, $S[P(X)] = -(3/8)\log(3/8) - (1/4)\log(1/4) - 3(1/8)\log(1/8) \approx 1.4942$. It quantifies the *temporal structural diversity* of a time series. If some ordinal patterns appear more frequently than others, the PE decreases, indicating that the signal is less random and more predictable. This allows to unveil hidden temporal information that helps to achieve a better understanding of the underlying dynamics. Technically speaking, the ordinal pattern probability distribution P is obtained once we fix the embedding dimension D and the embedding delay time τ. Taking into account that there are $D!$ potential permutations for a $D-$dimensional vector, the condition $N \gg D!$, with N the length of the time series, must be satisfied in order to obtain a reliable estimation of P [50]. For practical purposes, BP suggest in their seminal paper to estimate the frequency of ordinal patterns with $3 \leq D \leq 7$ and embedding delay $\tau = 1$ (consecutive points). It has been recently shown that the analysis of the PE as a function of τ may be particularly helpful for characterizing experimental time series on a wide range of temporal scales [32, 51]. By changing the value of the embedding delay τ different time scales are being considered because τ physically corresponds to multiples of the sampling time of the signal under analysis. For further details about the BP methodology, we recommend Refs. [51–53]. It is common to normalize the PE, and therefore in this paper, a normalized PE given by

$$\mathcal{H}_S[P] = S[P]/S_{\max} = S[P]/\log(D!) \tag{1}$$

is implemented, with $S_{\max} = \log(D!)$ the value obtained from an equiprobable ordinal pattern probability distribution. Defined in this way, $\mathcal{H}_S$ ranges between 0 and 1. The maximum value is obtained for a totally random stochastic process (white noise) while the minimum value is reached for a completely regular (monotonically increasing or decreasing) time series.

Since the BP approach symbolizes the series replacing the observable value by its corresponding rank in the sequence, the occurrence of equal values deserves a special handle. In the case of two elements in the vector having the same value, they are very often ranked by their temporal order. For example, a vector $(1, 4, 1)$, would be mapped to (021). This is the most commonly implemented recipe for dealing with ties. Another alternative, much more rarely used, is to add a small amount of observational noise to break equalities. The amplitude of the noise should be sufficiently small to not modify the ordinal relations in the data set, except for those vectors which have equal values. We insist on the fact that this latter approach has been applied in very few cases. We can cite Refs. [54, 55] as two of these rare exceptions. To the best of our knowledge, how the PE estimated values are affected by the occurrence of a high frequency of equal values in the original data has not been previously explored in detail. In an effort to fill this gap, we have included in the following two sections numerical and experimental tests for characterizing this PE limitation.

3. Numerical analysis

To illustrate the effect that the occurrence of a high frequency of ties has on PE estimated values, we have numerically generated an ensemble of one hundred independent sequences of $N = 1,000$ pseudorandom integer values drawn from a discrete uniform distribution on the interval $[0, i]$ with i ranging from 1 to 50 with step equal to one. The MATLAB function *randi* has been used for such a purpose. For more information about this function, we refer the interested reader to the following website: www.mathworks.com/help/matlab/ref/randi.html. In particular, when $i = 1$, pseudorandom uniform binary sequences of 0's and 1's are considered. Examples of these pseudorandom uniform discrete time series for $i = 1$, $i = 9$, and $i = 50$ are plotted in Fig. 1. Obviously, the number of ties is very large for the binary case, and it decreases as i increases.

The normalized PE (Eq. 1) with different embedding dimensions, $D \in \{3, 4, 5, 6\}$, and embedding delay $\tau = 1$ (consecutive data points) has been estimated for the one hundred independent realizations for each i-value. Mean and standard deviation (as error bars) are shown in Fig. 2 as a function of i. The normalized PE estimated values associated with continuous uniformly distributed pseudorandom numbers on the open interval $(0, 1)$, generated by implementing the *rand* function of MATLAB with a Mersenne Twister algorithm [56], have been also included. Being more precise, means from one hundred independent realizations of the same length ($N = 1,000$) for the different embedding dimension are indicated with horizontal dashed lines. It is clearly observed that normalized PE values from pseudorandom discrete time series with a high frequency of occurrence of equal values are much lower than those obtained for a pseudorandom continuous time series, leading to a totally spurious identification of non-random temporal structures. Because of the way ties are ordered, the relative frequencies of some permutation patterns are overestimated in detriment of those associated with other motifs which are underestimated, and, consequently, a non-uniform ordinal pattern probability distribution is obtained. This causes a decrease in the normalized PE estimation that could be erroneously interpreted as a signature of temporal correlation. Estimated PE values for the pseudorandom discrete simulations converge

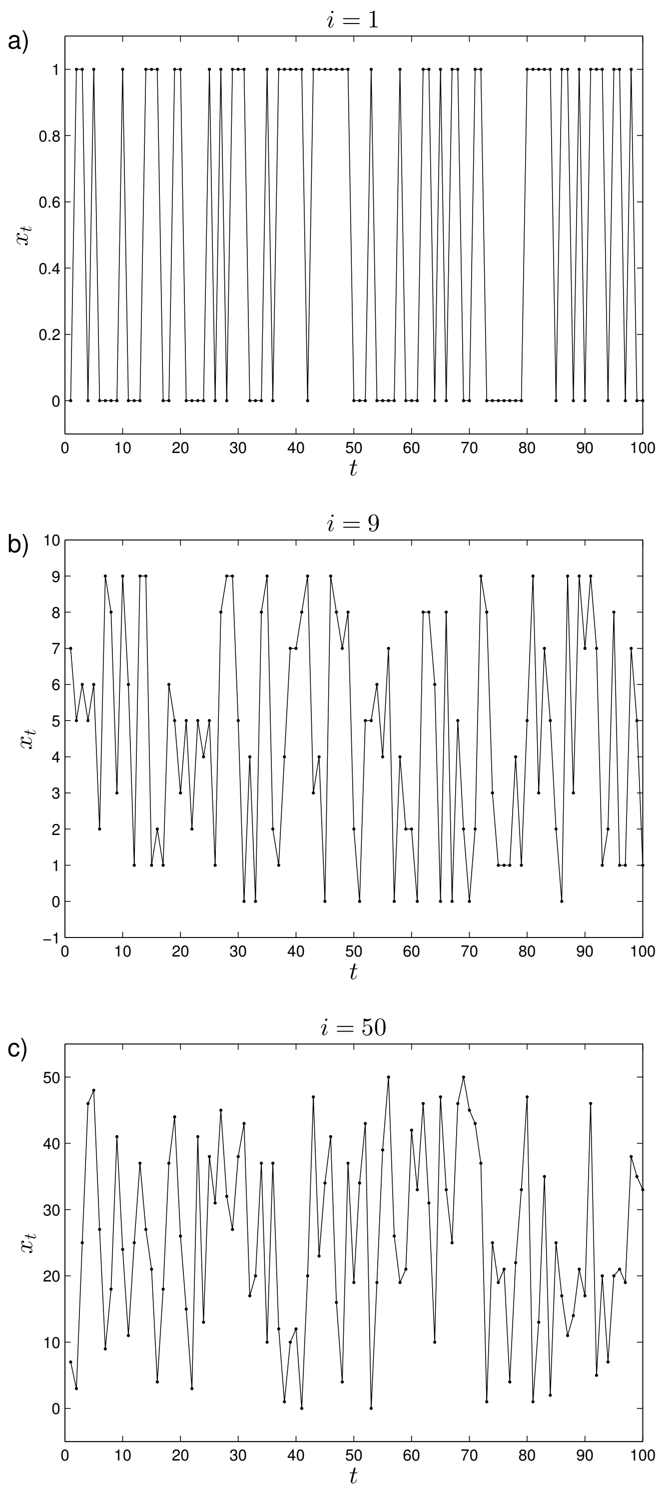

Figure 1: Some examples of the numerically generated discrete pseudorandom sequences. Integer values are drawn from a discrete uniform distribution on the interval $[0, i]$ with a) $i = 1$, b) $i = 9$, and c) $i = 50$. Only one hundred data points are depicted for a better visualization.

to those calculated for the pseudorandom continuous counterparts as the i-value increases. Analysis by implementing the WPE have been also carried out. For further details about this different definition of PE, that retains amplitude information, please see Ref. [43]. Results obtained, shown in Fig. 3, confirm that this improved ordinal permutation quantifier also suffers from this weakness.

We have found qualitative similar findings for larger time series ($N = 10,000$ data points) as it is observed in Fig. 4. Actually, the rate of convergence of the normalized PE estimations from the discrete to the continuous case is slower when longer time series are considered (please compare enlargements of Figs. 2 and 4). Besides, in another numerically controlled test, pseudorandom sequences of continuous (uniform, Gaussian and exponential) distributions have been discretized and analyzed. Behavior observed are qualitatively equivalent, *i.e.* once again the PE estimations decrease when the number of discretization levels decreases, suggesting (incorrectly) the presence of non-trivial dynamics. Interested readers can request these results by contacting the first author via e-mail. Finally, it is worth remarking here that the normalized PE and WPE estimated values for numerical realizations of continuous uniformly distributed pseudorandom numbers (horizontal dashed lines in Figs. 2-4) are lower than one due to finite-size effects. The offset increases as a function of the embedding dimension D and it decreases for larger time series lengths.

4. Real-world applications

4.1. Decimal expansion of irrational numbers

As a first real-world application, we are interested to investigate the randomness of the decimal expansion of irrational numbers by using the PE. We analyzed the ordinal pattern probability distribution of the temporal sequences obtained by picking the first 10,000 digits of the decimal expansion of several irrational numbers such as π, e, and $\sqrt{2}$. For illustrative purpose, we have plotted the first one hundred entries of these time series in Fig. 5. The relative frequencies of the ordinal patterns with different embedding dimensions, $D \in \{3, 4, 5, 6\}$, and embedding delay $\tau = 1$ for the sequences associated with these three

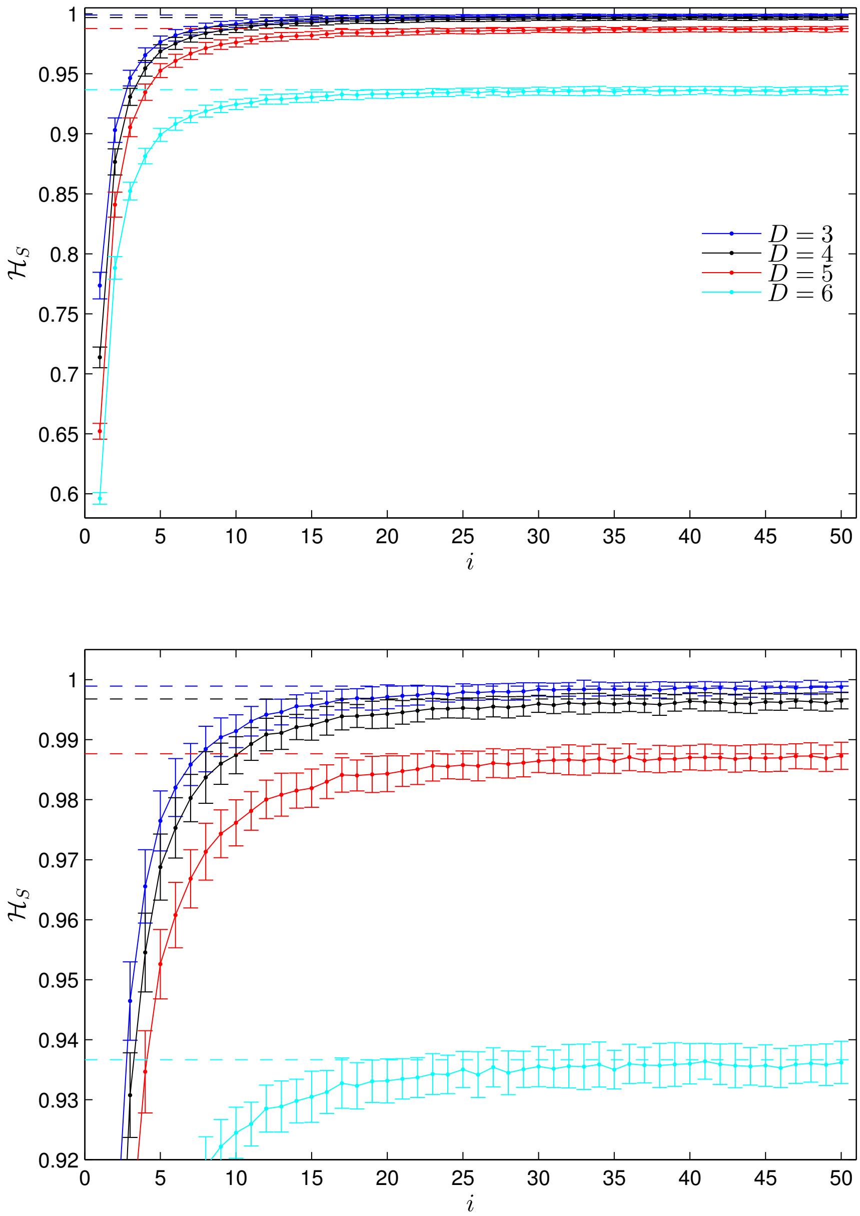

Figure 2: Top: Mean and standard deviation (as error bar) of $\mathcal{H}_S$ (Eq. 1) for one hundred independent realizations of $N = 1,000$ pseudorandom integer values drawn from a discrete uniform distribution on the interval $[0, i]$. Results obtained for different embedding dimensions ($D \in \{3, 4, 5, 6\}$) and embedding delay $\tau = 1$ are included. Horizontal dashed lines indicate the mean value of $\mathcal{H}_S$ for one hundred independent realizations of $N = 1,000$ pseudorandom numbers from a continuous uniform distribution. Bottom: Enlargement for a better view of the results obtained for lower discretization (larger values of i).

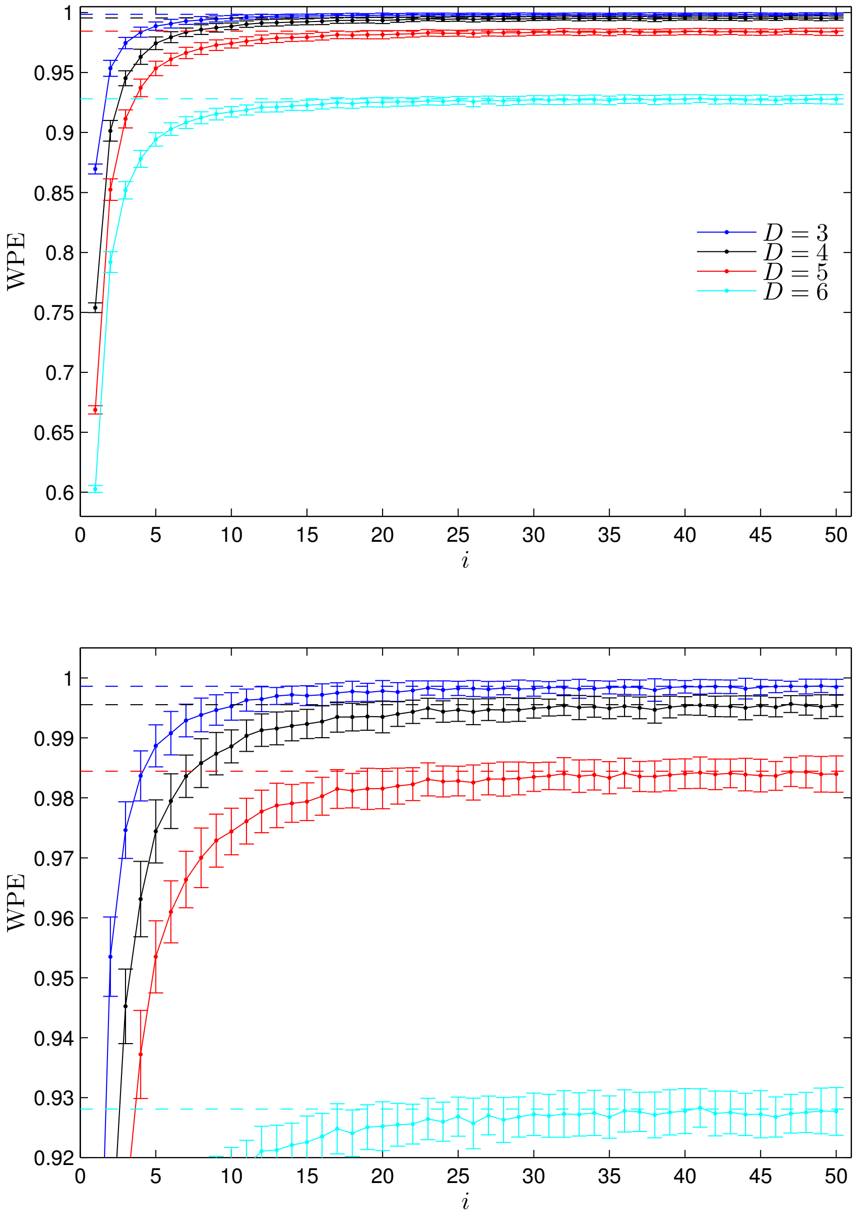

Figure 3: Same as Fig. 2 but using the normalized WPE, an improved PE better suited to characterize signals having considerable amplitude information.

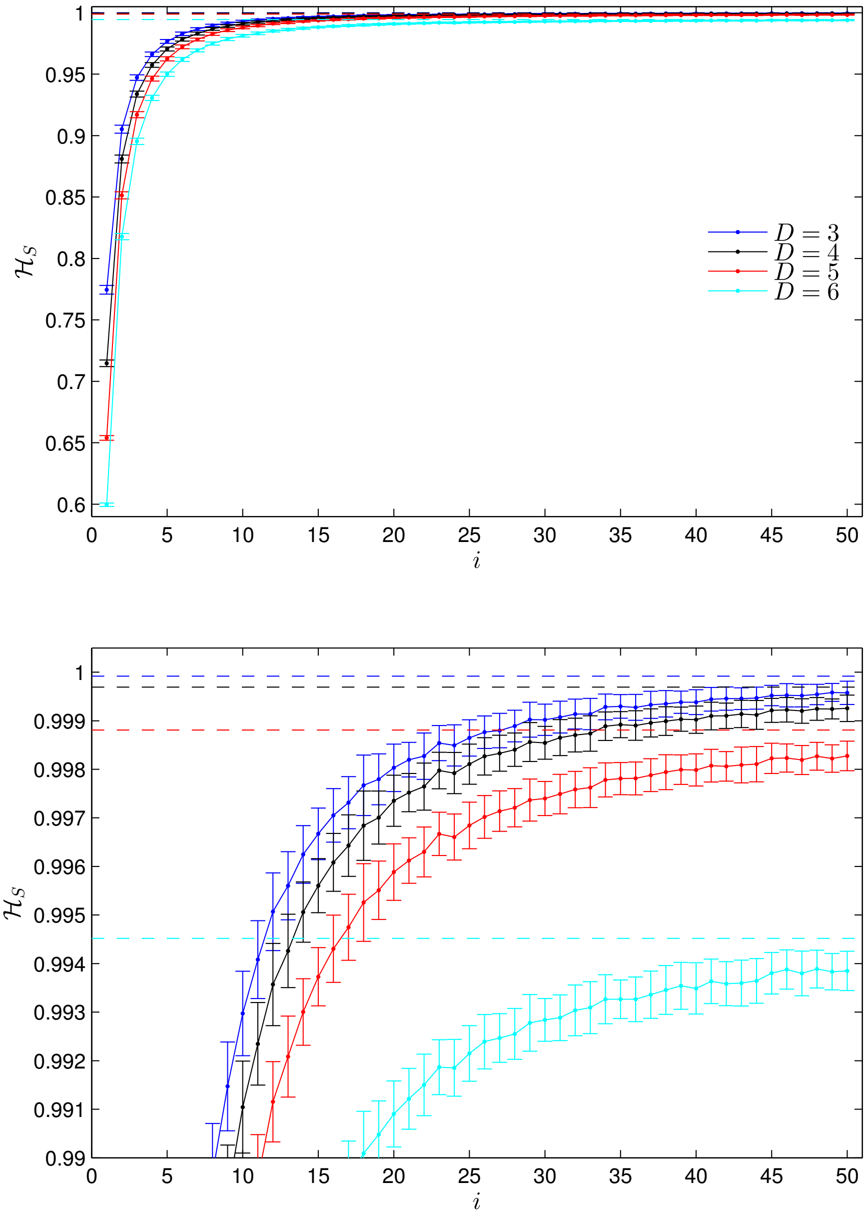

Figure 4: Same as Fig. 2 but for time series of length $N = 10,000$ data points.

irrational numbers are shown in Figs. 6-8. Ordinal patterns are numbered following the convention used by Parlitz *et al.* [51]. Figure 9 shows the indices associated with the ordinal patterns for $D = 3$ (top) and $D = 4$ (bottom). As it is visually concluded from Figs. 6-8, the different motifs are not equiprobable. Some of them are more probable than others, indicating, apparently, the presence of temporal complex structures in the data. But perhaps what is more intriguing is the fact that the relative frequencies of the ordinal patterns seem to be the same for the different irrational numbers. Consequently, the normalized PE estimated values are very similar as it is detailed in Table 1. Are these irregular ordinal patterns probability distributions due to true temporal correlations or can they be attributed to the occurrence of high frequencies of ties? In order to provide an answer to this question, we estimate the normalized PE of an ensemble of one hundred sequences of $N = 10,000$ pseudorandom integer values drawn from a discrete uniform distribution on the interval $[0, 9]$. The relative frequencies of the ordinal patterns for one arbitrarily chosen pseudorandom realization is shown in Fig. 10. It is worth pointing out here the strong similarity with the corresponding relative frequencies of the ordinal patterns obtained for the irrational numbers analysis (please compare Figs. 6-8 with Fig. 10). The mean and standard deviation of $\mathcal{H}_S$ for the one hundred pseudorandom realizations are detailed in Table 2. These results are consistent with those obtained from the sequences of irrational numbers, *i.e* the normalized PE estimations for π, e, and $\sqrt{2}$ (please see Table 1) lie inside the three standard deviations confidence interval ($\mu \pm 3\sigma$) obtained for the pseudorandom simulations (please see Table 2). Thus, the presence of true temporal correlations should be discarded. We have also carried out a surrogate analysis. More precisely, one thousand independent shuffled realizations have been generated for each one of the three irrational sequences. In the shuffled realizations, the values of the original series are permuted in a random way and, consequently, any potential temporal structure is destroyed. Results obtained are summarized in Fig. 11 where boxplots are used to display the distributions of normalized PE estimated values for the shuffled realizations. Since the normalized PE calculated for the original series overlap with those obtained for their shuffled counterparts, this surrogate analysis allows to confirm, once again, that the null hypothesis of randomness can not be rejected. This finding is in agreement

Table 1: Normalized PE values for the first 10,000 digits of the decimal expansion of π, e, and $\sqrt{2}$ with different embedding dimensions and embedding delay $\tau = 1$.

	$D=3$	$D=4$	$D=5$	$D=6$
π	0.992	0.990	0.986	0.978
e	0.992	0.989	0.986	0.978
$\sqrt{2}$	0.992	0.991	0.988	0.980

Table 2: Mean μ and standard deviation σ of $\mathcal{H}_S$ (Eq. 1) for one hundred sequences of $N = 10,000$ pseudorandom integer values drawn from a discrete uniform distribution on the interval $[0, 9]$ with different embedding dimensions and embedding delay $\tau = 1$.

	$D=3$	$D=4$	$D=5$	$D=6$
μ	0.991	0.989	0.986	0.979
σ	0.001	0.001	0.001	0.001

with results obtained by Luque *et al.* [57], who have implemented a totally different (complex network) approach. Our results also imply that the irregularly observed frequency of motifs is a totally spurious effect due to the significant number of equalities that is present in the original time series. Moreover, a surrogate analysis with shuffled realizations appears as a practical alternative to overcome this limitation of the PE.

4.2. Radioactive decay data

We have finally developed an ordinal symbolic analysis for radioactive decay data. Radioactive decay is a widely recognized natural source of random numbers [58]. We tested the alpha-activity of plutonium-239 (^{239}Pu, half-life: 24,110 years) looking for this expected random dynamics. A signal of length $N = 10,000$ ($\sim$ 2.8 hours) recorded at a sampling rate of 1 Hz by a shielded Geiger counter has been examined. A small segment of the whole record is shown in Fig. 12 and, once again, the occurrence of equalities in the time series is visually verified. The relative frequencies of the ordinal patterns for embedding dimension

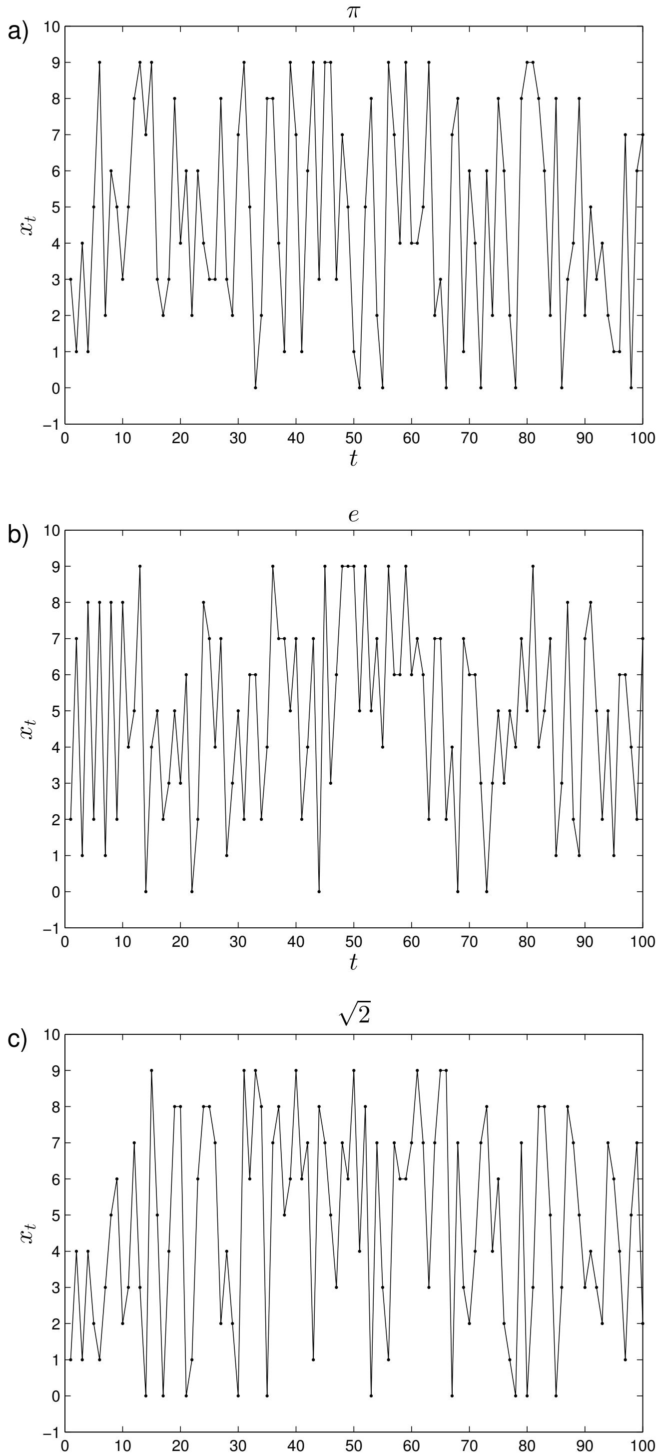

Figure 5: Sequences of digits associated with the decimal expansion of a) π, b) e, and c) $\sqrt{2}$. Only the first one hundred entries are shown for a better visualization.

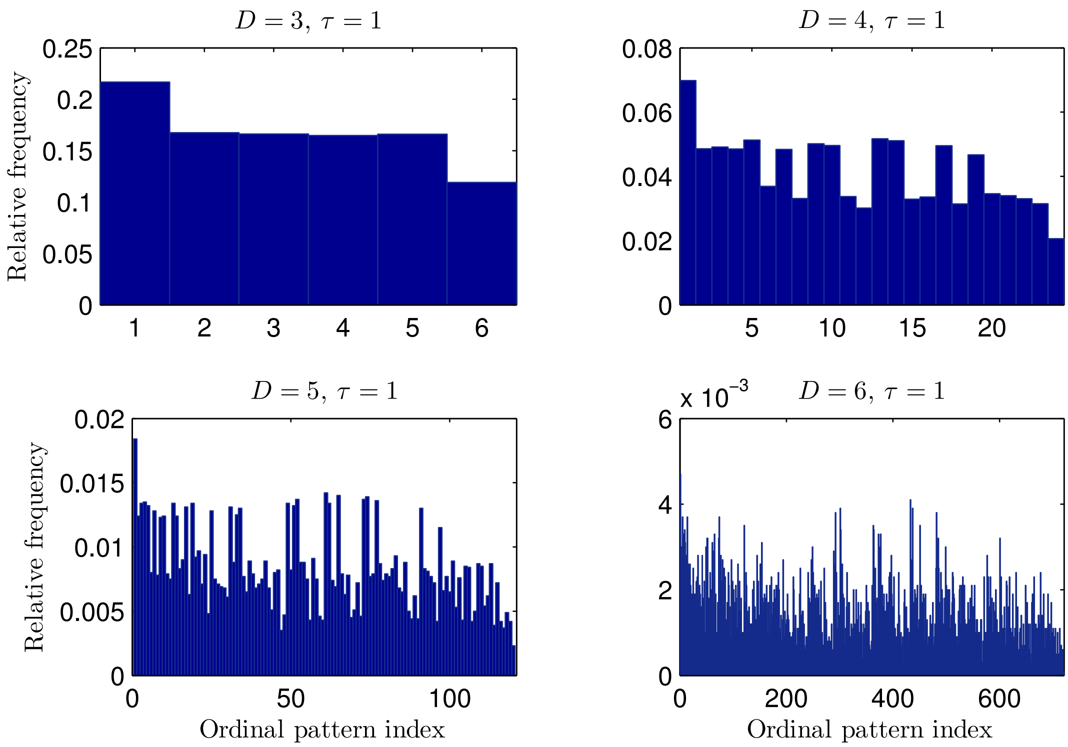

Figure 6: Relative frequencies of the ordinal patterns for the first 10,000 digits of the decimal expansion of π. Different embedding dimensions, $D \in \{3, 4, 5, 6\}$, and embedding delay $\tau = 1$ have been considered. Indices associated with motifs follow the convention used by Parlitz *et al.* [51].

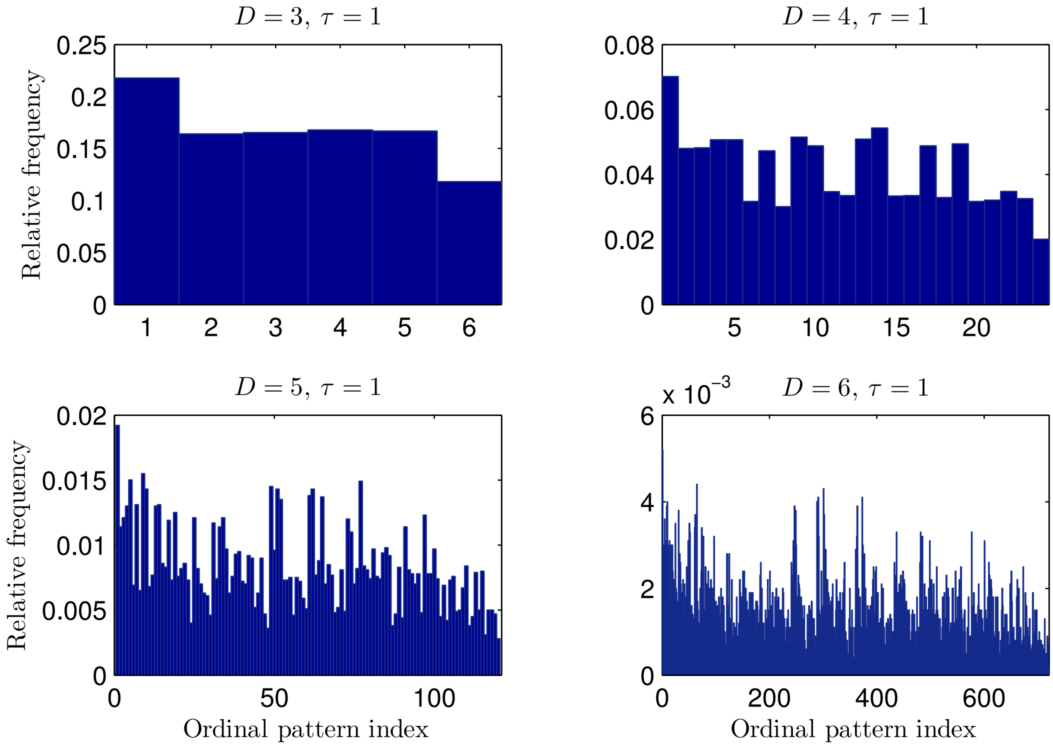

Figure 7: Same as Fig. 6 but for e.

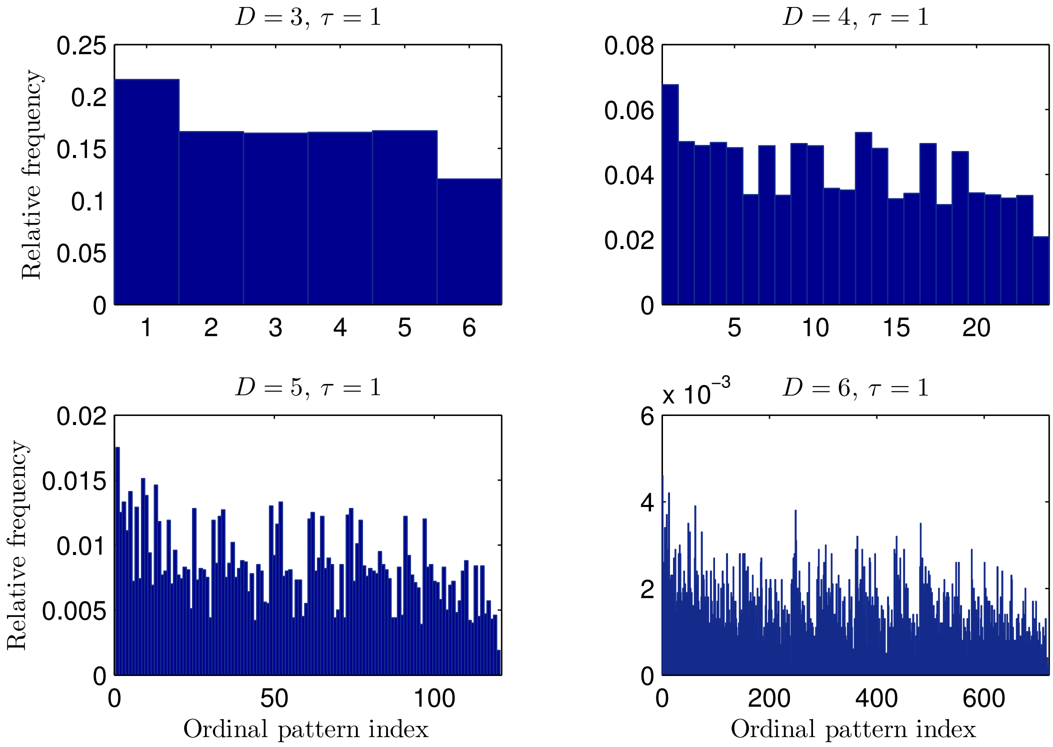

Figure 8: Same as Fig. 6 but for $\sqrt{2}$.

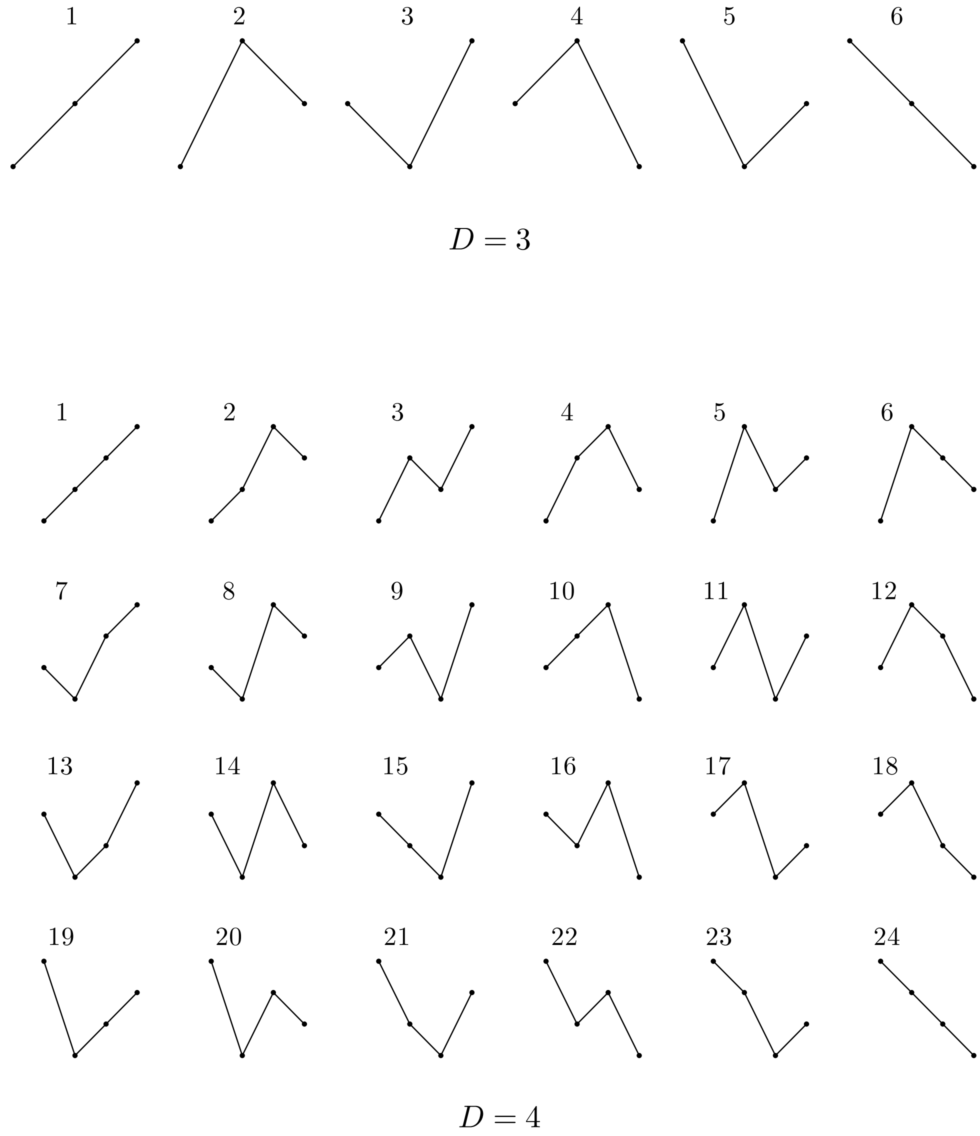

Figure 9: Ordinal patterns for $D = 3$ (top) and $D = 4$ (bottom) are depicted. They are numbered following the convention used by Parlitz *et al.* [51].

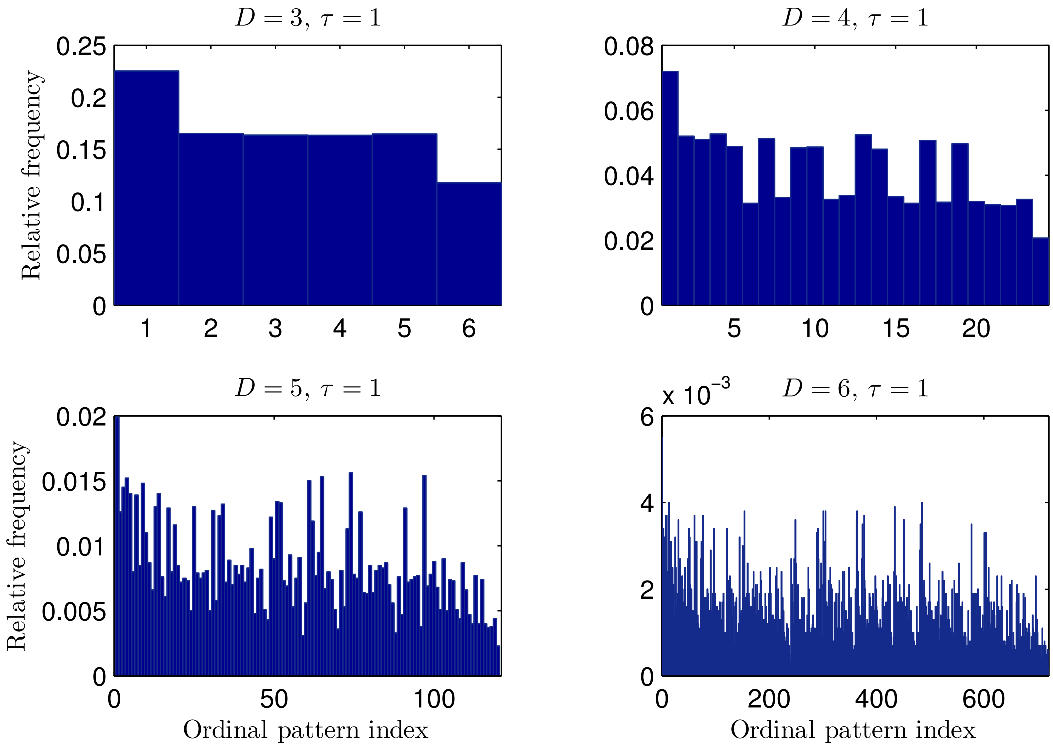

Figure 10: Same as Fig. 6 but for an arbitrarily chosen sequence of $N = 10,000$ pseudorandom integer values drawn from a discrete uniform distribution on the interval $[0, 9]$. Behaviors obtained for the other ninety-nine realizations are very similar.

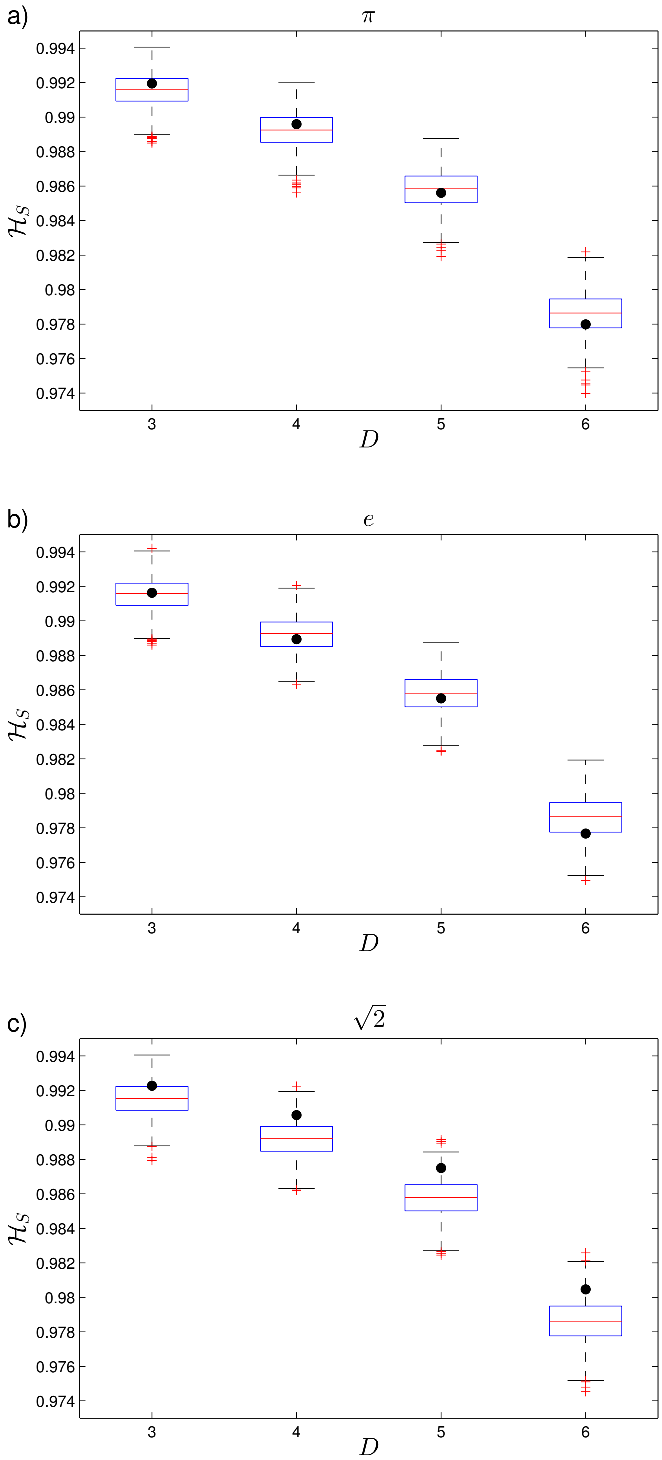

Figure 11: A surrogate data analysis with one thousand independent shuffled realizations for the first 10,000 digits of the decimal expansion of a) π, b) e, and c) $\sqrt{2}$. The normalized PE (Eq. 1) has been estimated with different embedding dimensions, $D \in \{3, 4, 5, 6\}$, and embedding delay $\tau = 1$. Black circles indicate the values estimated for the original time series while boxplots are used to display the distributions of estimated values for the shuffled realizations.

$D = 3$ and embedding delays τ between 1 and 100 are depicted in Fig. 13 a). In this case we have varied the embedding delay in order to check the behavior of the experimental data for different time scales, *i.e.* for different sampling times. It is concluded that, independently of the time scale, the ordinal pattern probability distribution is irregular. In fact, the motif indexed as 1 is clearly more frequent while motif labeled as 6 is less frequent in the temporal sequence. We have also included, in Fig. 13 b) and for comparison purpose, the relative frequencies of motifs associated with a sequence of $N = 10,000$ normally distributed pseudorandom numbers. As it was expected, in this continuous case, the six ordinal patterns are equiprobable independently of τ. These results could be taken as an astonishing proof of the presence of non-random structure in radioactive decay. In order to confirm or reject this early interpretation, a similar analysis with one thousand independent shuffled realizations of the original record has been performed. As it is shown in Fig. 14, irregular profiles are also obtained for the shuffled realizations. Hence, the randomness hypothesis can not be rejected. The initial apparent evidence of non-random temporal structure is thus a spurious effect due to the way equal values are handled with the BP algorithm.

5. Conclusions

In this paper, we have analyzed the incidence that a significant occurrence of equalities in the time series under study has on PE estimations. Through numerical analysis, it has been shown that PE obtained values are biased as a consequence of the presence of ties in the records. Equal values are usually ranked according to their order of appearance. This way of dealing with ties introduces non-negligible spurious temporal correlations that can potentially lead to erroneous conclusions about the true underlying dynamic nature. Particularly, we have found that lower PE values than those expected are estimated from highly discretized pseudorandom time series. We have also confirmed that experimentally recorded observables digitized with low sampling resolutions could be especially affected by this PE limitation. Some strategies to overcome this drawback have been discussed. Taking into account that the number of PE applications has increased a lot during the last years, we conjecture that our findings can be of help to reach a more reliable interpretation of results

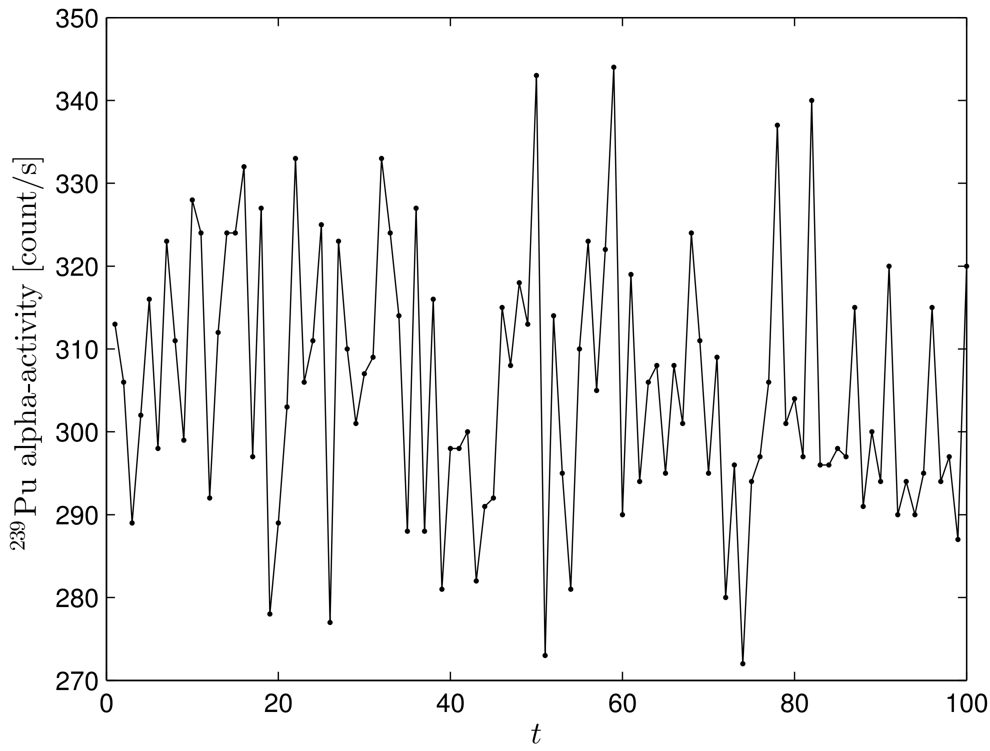

Figure 12: Alpha-activity of plutonium-239. A small segment of the whole record is shown for a better visualization.

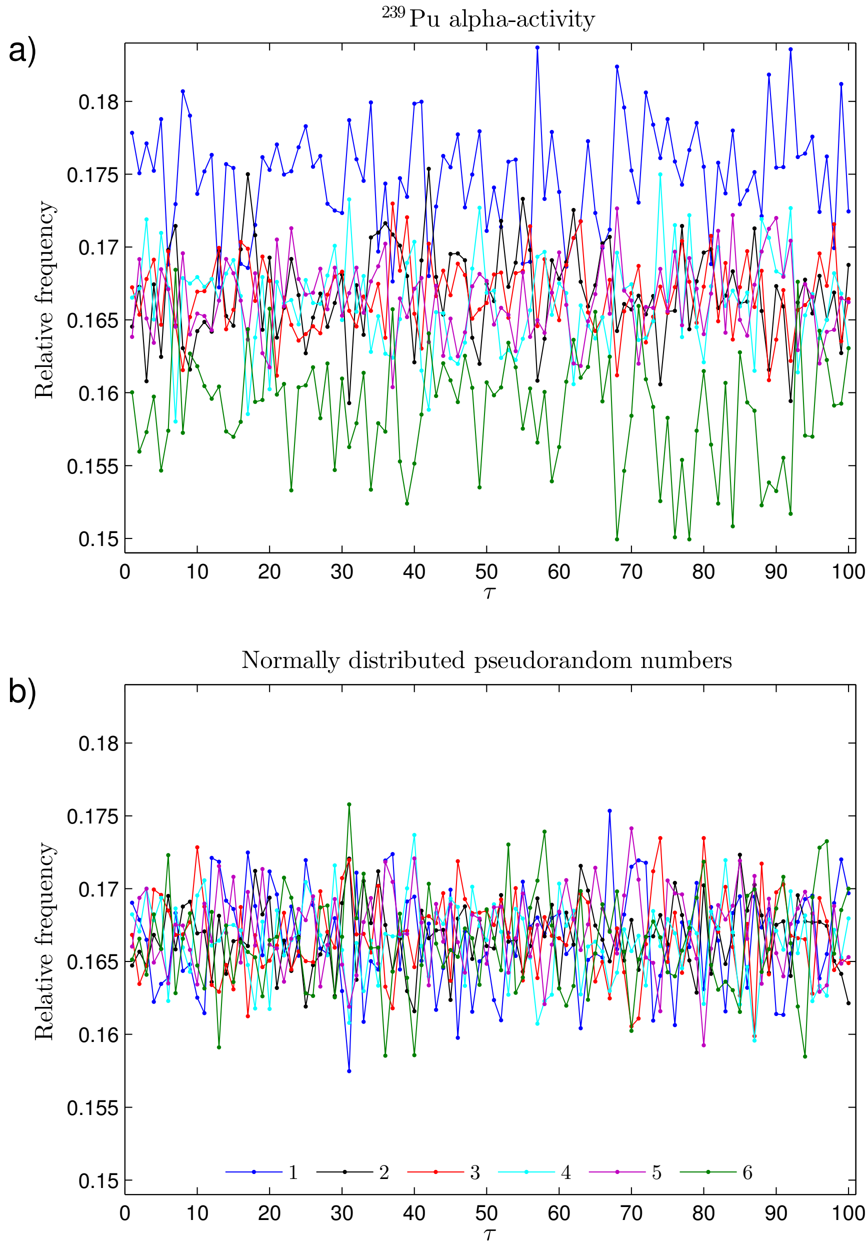

Figure 13: a) Relative frequencies of the ordinal patterns for the alpha-activity of plutonium-239 with $D = 3$ and $1 \leq \tau \leq 100$. Motifs are labeled following the convention displayed in Fig. 9 (top). b) The same analysis for a sequence of $N = 10,000$ normally distributed pseudorandom numbers.

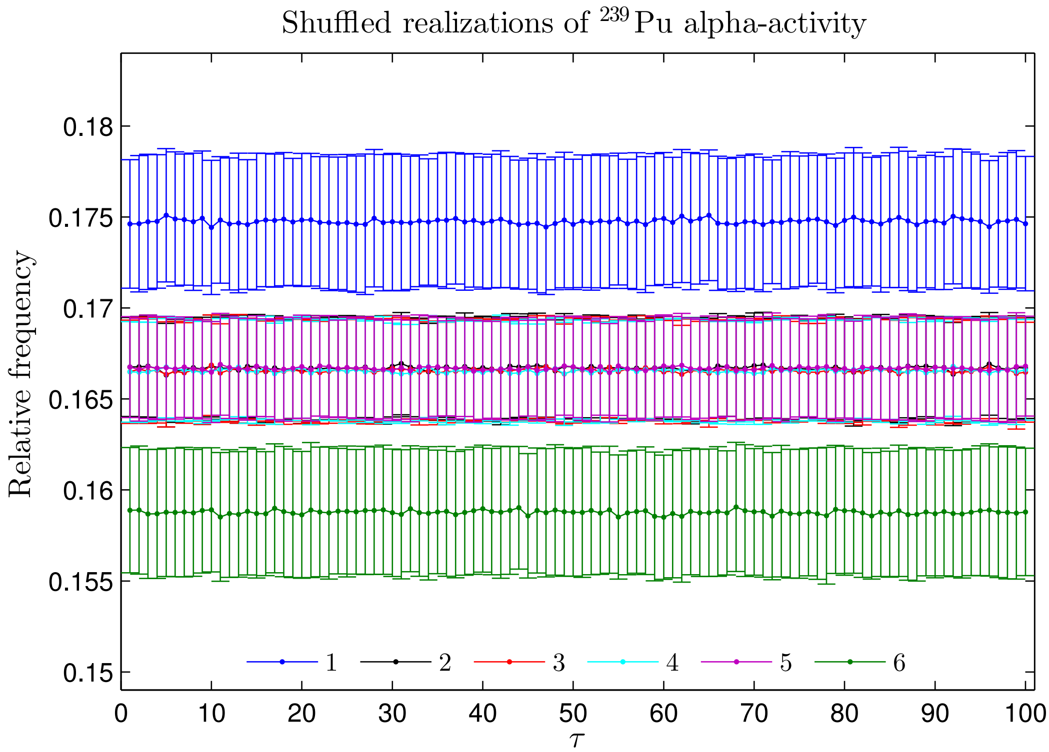

Figure 14: Relative frequencies of the ordinal patterns for one thousand independent shuffled realizations of the original ^{239}Pu alpha-activity record. Mean and standard deviation (as error bar) of the estimated probabilities with $D = 3$ and $1 \leq \tau \leq 100$ are shown.

when applying this information-theory-ordinal quantifier to experimentally acquired signals. Furthermore, our results might be also useful when using other quantifiers that implement the BP symbolic representation for characterizing experimental records.

Acknowledgements

We thank Prof. Simon E. Shnoll (Moscow State University, Moscow, and Russian Academy of Sciences, Pushchino) for providing us with the radioactive decay data and Prof. Alejandro Frery (Universidade Federal de Alagoas, Maceió, Alagoas, Brazil) for fruitful discussions about pseudorandom number generators. LZ and OAR gratefully acknowledge financial support from Consejo Nacional de Investigaciones Científicas y Técnicas (CONICET), Argentina. FO thanks support from Pontificia Universidad Católica de Valparaíso.

References

[1] C. Bandt, B. Pompe, Permutation entropy: A natural complexity measure for time series, Phys. Rev. Lett. 88 (17) (2002) 174102. doi:10.1103/PhysRevLett.88.174102.

[2] Y. Cao, W. W. Tung, J. B. Gao, V. A. Protopopescu, L. M. Hively, Detecting dynamical changes in time series using the permutation entropy, Phys. Rev. E 70 (4) (2004) 046217. doi:10.1103/PhysRevE.70.046217.

[3] X. Li, G. Ouyang, D. A. Richards, Predictability analysis of absence seizures with permutation entropy, Epilepsy Research 77 (1) (2007) 70–74. doi:10.1016/j.eplepsyres.2007.08.002.

[4] X. Li, S. Cui, L. J. Voss, Using permutation entropy to measure the electroencephalographic effects of sevoflurane, Anesthesiology 109 (3) (2008) 448–456. doi:10.1097/ALN.0b013e318182a91b.

[5] F. C. Morabito, D. Labate, F. La Foresta, A. Bramanti, G. Morabito, I. Palamara, Multivariate multi-scale permutation entropy for complexity analysis of Alzheimer's disease EEG, Entropy 14 (7) (2012) 1186–1202. doi:10.3390/e14071186.

[6] J. Li, J. Yan, X. Liu, G. Ouyang, Using permutation entropy to measure the changes in EEG signals during absence seizures, Entropy 16 (6) (2014) 3049–3061. doi:10.3390/e16063049.

[7] Z. Liang, Y. Wang, X. Sun, D. Li, L. J. Voss, J. W. Sleigh, S. Hagihira, X. Li, EEG entropy measures in anesthesia, Front. Comput. Neurosci. 9 (2015) 16. doi:10.3389/fncom.2015.00016.

[8] F. Montani, R. Baravalle, L. Montangie, O. A. Rosso, Causal information quantification of prominent dynamical features of biological neurons, Phil. Trans. R. Soc. A 373 (2056) (2015) 20150109. doi:10.1098/rsta.2015.0109.

[9] F. Montani, O. A. Rosso, F. S. Matias, S. L. Bressler, C. R. Mirasso, A symbolic information approach to determine anticipated and delayed synchronization in neuronal circuit models, Phil. Trans. R. Soc. A 373 (2056) (2015) 20150110. doi:10.1098/rsta.2015.0110.

[10] H. Azami, J. Escudero, Improved multiscale permutation entropy for biomedical signal analysis: Interpretation and application to electroencephalogram recordings, Biomed. Signal Process. Control 23 (2016) 28–41. doi:10.1016/j.bspc.2015.08.004.

[11] M. C. Soriano, L. Zunino, O. A. Rosso, I. Fischer, C. R. Mirasso, Time scales of a chaotic semiconductor laser with optical feedback under the lens of a permutation information analysis, IEEE J. Quantum Electron. 47 (2) (2011) 252–261. doi:10.1109/JQE.2010.2078799.

[12] L. Zunino, O. A. Rosso, M. C. Soriano, Characterizing the hyperchaotic dynamics of a semiconductor laser subject to optical feedback via permutation entropy, IEEE J. Sel. Top. Quantum Electron. 17 (5) (2011) 1250–1257. doi:10.1109/JSTQE.2011.2145359.

[13] J. P. Toomey, D. M. Kane, Mapping the dynamic complexity of a semiconductor laser with optical feedback using permutation entropy, Opt. Express 22 (2) (2014) 1713–1725. doi:10.1364/OE.22.001713.

[14] L. Yang, W. Pan, L. Yan, B. Luo, N. Li, Mapping the dynamic complexity and synchronization in unidirectionally coupled external-cavity semiconductor lasers using permutation entropy, J. Opt. Soc. Am. B 32 (7) (2015) 1463–1470. doi:10.1364/JOSAB.32.001463.

[15] H. Liu, B. Ren, Q. Zhao, N. Li, Characterizing the optical chaos in a special type of small networks of semiconductor lasers using permutation entropy, Opt. Commun. 359 (2016) 79–84. doi:10.1016/j.optcom.2015.09.059.

[16] H. Lange, O. A. Rosso, M. Hauhs, Ordinal pattern and statistical complexity analysis of daily stream flow time series, Eur. Phys. J. Spec. Top. 222 (2) (2013) 535–552. doi:10.1140/epjst/e2013-01858-3.

[17] F. Serinaldi, L. Zunino, O. A. Rosso, Complexity-entropy analysis of daily stream flow time series in the continental United States, Stoch. Env. Res. Risk Assess. 28 (7) (2014) 1685–1708. doi:10.1007/s00477-013-0825-8.

[18] T. Stosic, L. Telesca, D. V. de Souza Ferreira, B. Stosic, Investigating anthropically induced effects in streamflow dynamics by using permutation entropy and statistical complexity analysis: A case study, J. Hydrol. 540 (2016) 1136–1145. doi:10.1016/j.jhydrol.2016.07.034.

[19] P. M. Saco, L. C. Carpi, A. Figliola, E. Serrano, O. A. Rosso, Entropy analysis of the dynamics of El Niño/Southern Oscillation during the Holocene, Physica A 389 (21) (2010) 5022–5027. doi:10.1016/j.physa.2010.07.006.

[20] G. Consolini, P. De Michelis, Permutation entropy analysis of complex magnetospheric dynamics, J. Atmos. Solar Terr. Phys. 115-116 (2014) 25–31. doi:10.1016/j.jastp.2013.11.005.

[21] S. Sippel, H. Lange, M. D. Mahecha, M. Hauhs, P. Bodesheim, T. Kaminski, F. Gans, O. A. Rosso, Di-

agnosing the dynamics of observed and simulated ecosystem gross primary productivity with time causal information theory quantifiers, PLoS ONE 11 (10) (2016) e0164960. doi:10.1371/journal.pone.0164960.

[22] L. Zunino, M. Zanin, B. M. Tabak, D. G. Pérez, O. A. Rosso, Forbidden patterns, permutation entropy and stock market inefficiency, Physica A 388 (14) (2009) 2854–2864. doi:10.1016/j.physa.2009.03.042.

[23] L. Zunino, M. Zanin, B. M. Tabak, D. G. Pérez, O. A. Rosso, Complexity-entropy causality plane: A useful approach to quantify the stock market inefficiency, Physica A 389 (9) (2010) 1891–1901. doi:10.1016/j.physa.2010.01.007.

[24] A. F. Bariviera, M. B. Guercio, L. B. Martinez, O. A. Rosso, The (in)visible hand in the Libor market: an information theory approach, Eur. Phys. J. B 88 (2015) 208. doi:10.1140/epjb/e2015-60410-1.

[25] A. F. Bariviera, M. B. Guercio, L. B. Martinez, O. A. Rosso, A permutation information theory tour through different interest rate maturities: the Libor case, Phil. Trans. R. Soc. A 373 (2056) (2015) 20150119. doi:10.1098/rsta.2015.0119.

[26] R. Yan, Y. Liu, R. X. Gao, Permutation entropy: A nonlinear statistical measure for status characterization of rotary machines, Mech. Syst. Signal Process. 29 (2012) 474–484. doi:10.1016/j.ymssp.2011.11.022.

[27] A. L. L. Aquino, T. S. G. Cavalcante, E. S. Almeida, A. C. Frery, O. A. Rosso, Characterization of vehicle behavior with information theory, Eur. Phys. J. B 88 (2015) 257. doi:10.1140/epjb/e2015-60384-x.

[28] A. L. L. Aquino, H. S. Ramos, A. C. Frery, L. P. Viana, T. S. G. Cavalcante, O. A. Rosso, Characterization of electric load with Information Theory quantifiers, Physica A 465 (2017) 277–284. doi:10.1016/j.physa.2016.08.017.

[29] F. O. Redelico, F. Traversaro, N. Oyarzabal, I. Vilaboa, O. A. Rosso, Evaluation of the status of rotary machines by time causal Information Theory quantifiers, Physica A 470 (2017) 321–329. doi:10.1016/j.physa.2016.05.031.

[30] O. A. Rosso, R. Ospina, A. C. Frery, Classification and verification of handwritten signatures with time causal information theory quantifiers, PLoS ONE 11 (12) (2016) e0166868. doi:10.1371/journal.pone.0166868.

[31] O. A. Rosso, H. A. Larrondo, M. T. Martín, A. Plastino, M. A. Fuentes, Distinguishing noise from chaos, Phys. Rev. Lett. 99 (15) (2007) 154102. doi:10.1103/PhysRevLett.99.154102.

[32] L. Zunino, M. C. Soriano, O. A. Rosso, Distinguishing chaotic and stochastic dynamics from time series by using a multiscale symbolic approach, Phys. Rev. E 86 (4) (2012) 046210. doi:10.1103/PhysRevE.86.046210.

[33] A. Bahraminasab, F. Ghasemi, A. Stefanovska, P. E. McClintock, H. Kantz, Direction of coupling from phases of interacting oscillators: a permutation information approach, Phys. Rev. Lett. 100 (8) (2008)

084101. doi:10.1103/PhysRevLett.100.084101.
[34] M. Staniek, K. Lehnertz, Symbolic transfer entropy, Phys. Rev. Lett. 100 (15) (2008) 158101. doi:10.1103/PhysRevLett.100.158101.
[35] L. Zunino, D. G. Pérez, A. Kowalski, M. T. Martín, M. Garavaglia, A. Plastino, O. A. Rosso, Fractional Brownian motion, fractional Gaussian noise, and Tsallis permutation entropy, Physica A 387 (24) (2008) 6057–6068. doi:10.1016/j.physa.2008.07.004.
[36] X. Zhao, P. Shang, J. Huang, Permutation complexity and dependence measures of time series, Europhys. Lett. 102 (4) (2013) 40005. doi:10.1209/0295-5075/102/40005.
[37] N. Mammone, J. Duun-Henriksen, T. W. Kjaer, F. C. Morabito, Differentiating interictal and ictal states in childhood absence epilepsy through permutation Rényi entropy, Entropy 17 (7) (2015) 4627–4643. doi:10.3390/e17074627.
[38] A. M. Unakafov, K. Keller, Conditional entropy of ordinal patterns, Physica D 269 (2014) 94–102. doi:10.1016/j.physd.2013.11.015.
[39] L. Zunino, F. Olivares, O. A. Rosso, Permutation min-entropy: An improved quantifier for unveiling subtle temporal correlations, Europhys. Lett. 109 (1) (2015) 10005. doi:10.1209/0295-5075/109/10005.
[40] C. Su, Z. Liang, X. Li, D. Li, Y. Li, M. Ursino, A comparison of multiscale permutation entropy measures in on-line depth of anesthesia monitoring, PLoS ONE 11 (10) (2016) 10.1371/journal.pone.0164104. doi:10.1371/journal.pone.0164104.
[41] J. P. Toomey, A. Argyris, C. McMahon, D. Syvridis, D. M. Kane, Time-scale independent permutation entropy of a photonic integrated device, J. Lightwave Technol. (In press). doi:10.1109/JLT.2016.2626387.
[42] C. Bian, C. Qin, Q. D. Y. Ma, Q. Shen, Modified permutation-entropy analysis of heartbeat dynamics, Phys. Rev. E 85 (2) (2012) 021906. doi:10.1103/PhysRevE.85.021906.
[43] B. Fadlallah, B. Chen, A. Keil, J. Príncipe, Weighted-permutation entropy: A complexity measure for time series incorporating amplitude information, Phys. Rev. E 87 (2) (2013) 022911. doi:10.1103/PhysRevE.87.022911.
[44] E. M. Bollt, T. Stanford, Y.-C. Lai, K. Życzkowski, Validity of threshold-crossing analysis of symbolic dynamics from chaotic time series, Phys. Rev. Lett. 85 (16) (2000) 3524–3527. doi:10.1103/PhysRevLett.85.3524.
[45] J. M. Amigó, K. Keller, V. A. Unakafova, Ordinal symbolic analysis and its application to biomedical recordings, Phil. Trans. R. Soc. A 373 (2034) (2015) 20140091. doi:10.1098/rsta.2014.0091.
[46] A. Aragoneses, N. Rubido, J. Tiana-Alsina, M. C. Torrent, C. Masoller, Distinguishing signatures of determinism and stochasticity in spiking complex systems, Sci. Rep. 3 (2013) 1778. doi:10.1038/srep01778.
[47] A. Aragoneses, T. Sorrentino, S. Perrone, D. J. Gauthier, M. C. Torrent, C. Masoller, Experimental

and numerical study of the symbolic dynamics of a modulated external-cavity semiconductor laser, Opt. Express 22 (4) (2014) 4705–4713. doi:10.1364/OE.22.004705.

[48] A. Aragoneses, L. Carpi, N. Tarasov, D. Churkin, M. Torrent, C. Masoller, S. Turitsyn, Unveiling temporal correlations characteristic of a phase transition in the output intensity of a fiber laser, Phys. Rev. Lett. 116 (3) (2016) 033902. doi:10.1103/PhysRevLett.116.033902.

[49] D. J. Little, D. M. Kane, Permutation entropy of finite-length white-noise time series, Phys. Rev. E 94 (2) (2016) 022118. doi:10.1103/PhysRevE.94.022118.

[50] M. Staniek, K. Lehnertz, Parameter selection for permutation entropy measurements, Int. J. Bifurcat. Chaos 17 (10) (2007) 3729–3733. doi:10.1142/S0218127407019652.

[51] U. Parlitz, S. Berg, S. Luther, A. Schirdewan, J. Kurths, N. Wessel, Classifying cardiac biosignals using ordinal pattern statistics and symbolic dynamics, Comput. Biol. Med. 42 (3) (2012) 319–327. doi:10.1016/j.compbiomed.2011.03.017.

[52] M. Zanin, L. Zunino, O. A. Rosso, D. Papo, Permutation entropy and its main biomedical and econophysics applications: A review, Entropy 14 (8) (2012) 1553–1577. doi:10.3390/e14081553.

[53] M. Riedl, A. Müller, N. Wessel, Practical considerations of permutation entropy. A tutorial review, Eur. Phys. J. Special Topics 222 (2) (2013) 249–262. doi:10.1140/epjst/e2013-01862-7.

[54] C. Quintero-Quiroz, S. Pigolotti, M. C. Torrent, C. Masoller, Numerical and experimental study of the effects of noise on the permutation entropy, New J. Phys. 17 (2015) 093002. doi:10.1088/1367-2630/17/9/093002.

[55] F. Olivares, L. Zunino, O. A. Rosso, Quantifying long-range correlations with a multiscale ordinal pattern approach, Physica A 445 (2016) 283–294. doi:10.1016/j.physa.2015.11.015.

[56] M. Matsumoto, T. Nishimura, Mersenne twister: a 623-dimensionally equidistributed uniform pseudo-random number generator, ACM Transactions on Modeling and Computer Simulation 8 (1) (1998) 3–30. doi:10.1145/272991.272995.

[57] B. Luque, L. Lacasa, F. Ballesteros, J. Luque, Horizontal visibility graphs: Exact results for random time series, Phys. Rev. E 80 (4) (2009) 046103. doi:10.1103/PhysRevE.80.046103.

[58] P. E. Rapp, A. M. Albano, I. D. Zimmerman, M. A. Jiménez-Montao, Phase-randomized surrogates can produce spurious identifications of non-random structure, Phys. Lett. A 192 (1) (1994) 27–33. doi:10.1016/0375-9601(94)91010-3.